Cancer Letters 456 (2019) 49–58

Contents lists available at ScienceDirect

Cancer Letters

journal homepage: www.elsevier.com/locate/canlet

Original Articles

Targeting the deubiquitinase STAMBPL1 triggers apoptosis in prostate cancer cells by promoting XIAP degradation

Xi Chen[a], Hongzhe Shi[a], Xingang Bi[a], Yajian Li[a], Zhenhua Huang[b,*]

[a] Department of Urology, National Cancer Center, National Clinical Research Center For Cancer, Cancer Hospital, Chinese Academy of Medical Sciences and Peking Union Medical College, Beijing, 100021, China

[b] Department of Oncology, Nanfang Hospital, Southern Medical University, Guangzhou, 510515, China

ARTICLE INFO

Keywords:
Deubiquitination
Inhibitor of apoptosis proteins
Proteasome
Lysosomal degradation

ABSTRACT

The zinc metalloprotease STAM-binding protein-like 1 (STAMBPL1) has been identified as a deubiquitinase by specifically cleaving Lys-63-linked polyubiquitin chains, but its cellular function remains unclear. Here we described the potential role of STAMBPL1 in suppression of the intrinsic apoptosis. We observed substantially high amounts of STAMBPL1 proteins in androgen-independent prostate cancer PC3 and DU145 cell lines. STAMBPL1 RNAi depletion triggered caspase-3/-7-dependent apoptosis in PC3 and DU145 cells. STAMBPL1 knockdown-induced apoptosis was accompanied by accumulation of cellular ROS and a decrease in endogenous caspase inhibitor XIAP protein content. Treatment cells with antioxidant NAC delayed STAMBPL1 silencing-induced apoptosis, whereas ectopic expression of XIAP almost completely abrogated apoptosis. We further elucidated that STAMBPL1 knockdown diverted XIAP protein to lysosomal degradation pathway. Taken together, these studies show that STAMBPL1 depletion induces apoptosis by promoting XIAP lysosomal degradation, and suggest that targeting deubiquitinase STAMBPL1 might offer promising therapeutic strategy for prostate cancer.

1. Introduction

Protein ubiquitination is a reversible process that has been shown to modulate a variety of biological events [1]. Upon activation, ubiquitin is covalently attached to target protein lysine residues. Multiple ubiquitin molecules can be linked to each other, thus generate polyubiquitin chains. Structurally different polyubiquitin chains guide proteins for different fates [1,2]. For instance, Lys 48-linked polyubiquitin chains serve as protein proteasomal degradation signal; while Lys 63-linked polyubiquitin chains involve in cell surface receptor internalization and endosomal sorting [3,4].

STAMBPL1 (also known as AMSH-LP) is a zinc dependent deubiquitinase, which specifically cleaves Lys 63-linked polyubiquitin chains [5,6]. Previous studies suggested that STAMBPL1 enhances the trafficking of EGFR to the cell surface by removing Lys 63-linked polyubiquitin chains [5,7,8]. However, its cellular function is not understood. Here we show evidence that STAMBPL1 regulates X-linked inhibitor of apoptosis protein (XIAP) stability, thus modulates apoptosis in prostate cancer cells.

XIAP is one of the Inhibitor of Apoptosis Protein family members that target apoptotic-caspase cascade [9]. XIAP contains three N-terminal baculovirus IAP repeat (BIR) domains, an ubiquitin-associated domain (UBA), followed by a C-terminal RING domain with E3 ubiquitin ligase activity. The BIR domains bind caspase-3/-7 or −9, and directly block their proteolytic activity, thus tightly modulate caspase activation. UBA domain binds to single ubiquitin as well as polyubiquitin chains which render protein proper function in various signaling process [3]. XIAP was found to be overexpressed in an array of human cancers, and XIAP protein level is inversely correlated with the sensitivity to apoptotic stimuli [10,11]. Therefore, inhibition of XIAP has become a promising application for cancer therapy.

Prostate cancer is the most common cancer in American men [12], and has become the fastest growing male malignancy diagnosed in China [13,14]. Almost all prostate cancers at initial stages of development are androgen-dependent, androgen ablation therapy could effective suppress tumor growth [15,16]. However, some cancerous cells gradually acquire resistance during this treatment, ultimately leading to androgen-refractory prostate cancer. Growing evidence showed that the progress to androgen-independent state is accompanied by the emergence of apoptosis-resistant cells [17,18]. Therefore, understanding the abnormalities in apoptosis pathway will contribute to the design of novel strategy for further therapy of prostate cancer.

In the present study, we observed the elevated STANBPL1 protein levels in androgen-independent prostate cancer PC3 and DU145 cells. We demonstrated that STAMBPL1 RNAi depletion induced apoptosis in

* Corresponding author.
E-mail address: happygao@smu.edu.cn (Z. Huang).

https://doi.org/10.1016/j.canlet.2019.04.020
Received 29 November 2018; Received in revised form 14 April 2019; Accepted 15 April 2019

PC3 and DU145 cells by promoting XIAP lysosomal degradation. Our results suggest that STAMBPL1 is a potential therapeutic target for prostate cancer.

2. Materials and methods

2.1. Cell culture and reagents

Human prostate carcinoma DU145, PC3, LNCaP, C4-2 and 22RV1 cells were cultured in regular RPMI 1640 medium containing 10% fetal bovine serum, 100 U/ml penicillin, and 100 μg of streptomycin. For the anti-androgen experiments, LNCaP cells were grown in androgen-depleted medium, phenol red-free RPMI 1640 supplemented with 5% charcoal-stripped FBS (Gibco) for 24 h and challenged with enzalutamide. Human prostatic epithelial RWPE-1 cells were grown in keratinocyte serum free medium supplemented with 0.05 mg/ml bovine pituitary extract and 5 ng/ml epidermal growth factor [19] (Gibco). Cell viability was measured by trypan blue exclusion assay. All

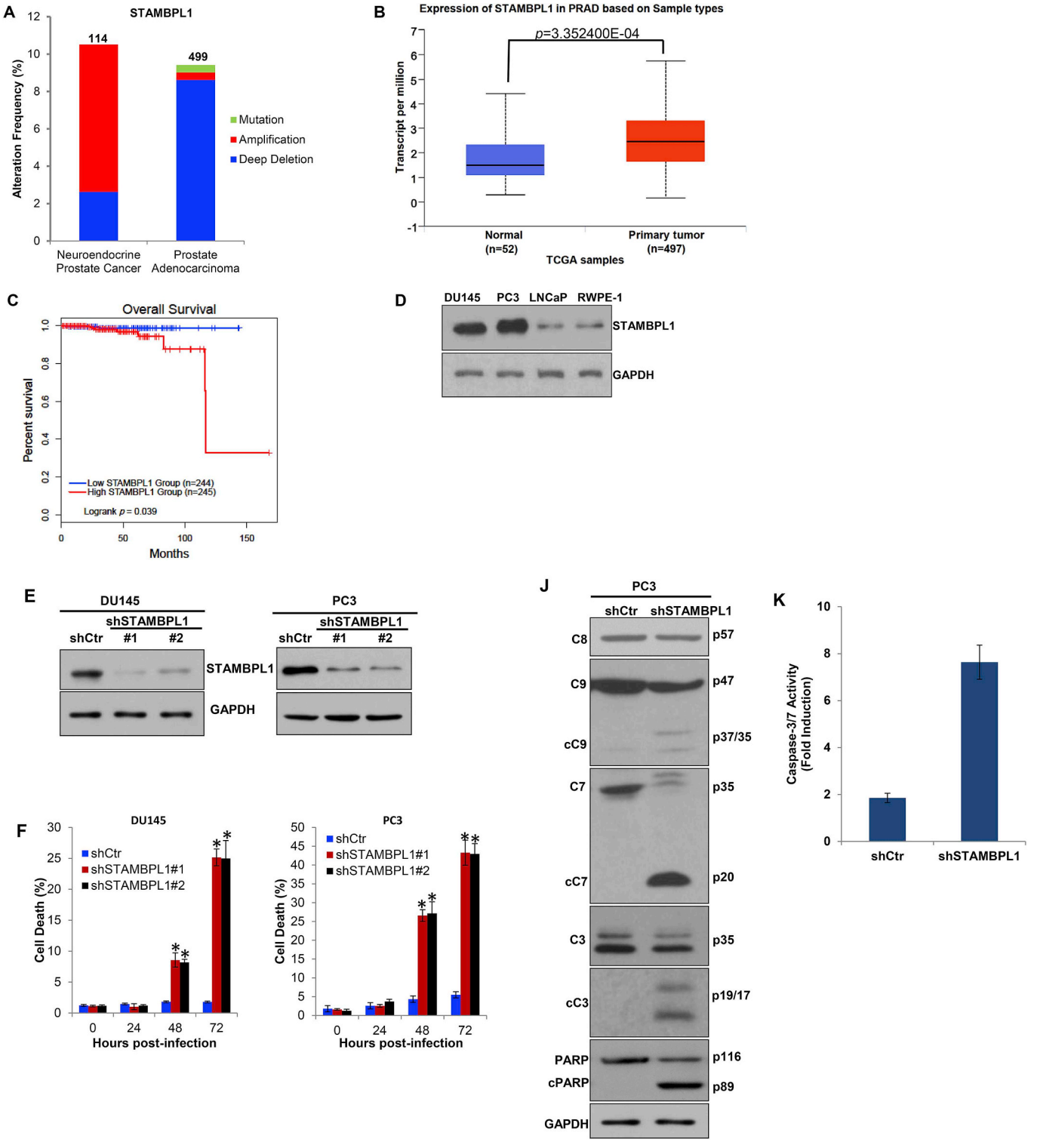

(caption on next page)

Fig. 1. Silencing of STAMBPL1 induces apoptosis.
A. Genetic alteration of STAMBPL1 in human prostate cancers retrieved from TCGA (http://www.cbioportal.org). Percentages of gene mutation, amplification (more copies) and deep deletion (copy number loss) are shown. The number of sample size is indicated on the top of each bar.
B. Boxplot showing the relative expression of STAMBPL1 gene in normal and prostate adenocarcinoma (PRAD) samples obtained from the TCGA database.
C. Kaplan-Meier overall survival rate of prostate adenocarcinoma was analyzed based on the TCGA data. *P*-value was calculated by Logrank test.
D. DU145, PC3, LNCaP and RWPE-1 cells were lysed and analyzed for STAMBPL1 expression by immunoblotting. GAPDAH was served as internal control for protein loading.
E. Immunoblotting analysis showing STAMBPL1 and GAPDH in DU145 and PC3 cells infected with control shRNA or shRNAs against STAMBPL1 (#1 and #2) for 2 days.
F. Depletion of STAMBPL1 induced DU145 and PC3 cell death as assessed by propidium iodide (PI) exclusion assay. Values are means ± SD of triplicates.
G. PC3 and DU145 cells were infected with control shRNA or STAMBPL1 shRNA for 24 h. Cells were treated with or without 20 μM of necrostatin-1 (Nec-1), chloroquine (CQ) or z-DEVD-FMK for 24 h. Cell death was analyzed by PI exclusion assay.
H. PC3 and DU145 cells were infected with control shRNA or shRNA against STAMBPL1 lentivirus for 72 h. Apoptosis were determined by Annexin V/PI staining followed by flow cytometry analysis.
I. PC3 and DU145 cells were treated as in E. DNA content analysis was performed to determine subG1 peak.
J. PC3 cells were treated as in E. Cells were lysed and analyzed by IB.
K. PC3 cells were infected with control shRNA or STAMBPL1 shRNA lentivirus for 48 h. Cells were assayed for caspase-3/7 activity.

cells were maintained in humidified incubator at 37 °C and 5% CO_2. Necrostatin-1 (Nec-1), Z-DEVD-FMK, Z-IETD-FMK, chloroquine (CQ) and enzalutamide were obtained from Selleckchem; N-acetyl cysteine (NAC), ferrostatin-1 (Fer-1), MG132, and leupeptin were from Sigma. H_2DCFDA, C11-BODIPY (581/591), and MitoSOX RED were from Molecular Probes, Invitrogen.

2.2. Gene expression profiling interaction analysis (GEPIA)

GEPIA (http://gepia.cancer-pku.cn/) is a web-based platform to profile gene expressions between normal and tumor tissues and to explore correlations between gene expression and cancer patient survival. It provides survival data for 9,763 patients from 33 cancer studies performed by The Cancer Genome Atlas (TCGA), along with RNA-Seq data for mRNAs from TCGA [20]. In this study, the GEPIA online tool was used to analyze the levels of STAMBPL1 between normal prostate tissues and primary prostate cancer tissues. The Kaplan-Meier overall survival curve of prostate cancer patients for STAMBPL1 gene was generated by GEPIA using a standard processing pipeline. We divided 489 prostate adenocarcinoma patients into low STAMBPL1 and high STAMBPL1 expression groups according to the median value.

2.3. RNAi and constructs

All transfections for siRNAs were performed using Lipofectamine RNAiMAX (Invitrogen) according to the manufacturer's protocol. pLenti-shCtr, and pLenti-shSTAMBPL1 were constructed using the Gateway cloning system (Invitrogen). Lentiviruses were produced in HEK293T cells by transfecting shRNA constructs along with packaging constructs (pol/gag and VSVG). The siRNA target sequence for the human caspase-8 gene is 5′- GATCAGAATTGAGGTCTTT- 3'. shSTAMBPL1#1: 5′- GAAAAGCTTCCTAACCATC-3'; shSTAMBPL1#2: 5′-GGTTGTAATATCACCATCA-3'. Adenovirus encoding Flag-XIAP was prepared as described previously [21].

2.4. Luciferase reporter assay

Cells in 96-well plates were transfected with a NF-κB firefly luciferase reporter plasmid using Lipofectamine Plus. Luciferase activity was determined in cell extracts using the Pierce Gaussia luciferase flash assay kit.

2.5. Western blotting and immunoprecipitation analysis

Cells were pelleted and lysed in RIPA buffer (25 mM Tris-HCl, pH = 7.5, 150 mM NaCl, 0.1% Nonidet P-40, 0.5% sodium deoxycholate and 0.1% SDS) supplemented with protease inhibitor cocktail (Sigma) and phosphatase Inhibitor Cocktail 2 and 3 (Sigma). The lysates were cleared by centrifugation at 12000 rpm for 10min. Nuclear protein fraction was obtained using the NE-PER nuclear and cytoplasmic extraction kit (Thermo Scientific). For immunoprecipitation, cells were lysed in RIPA buffer with the isopeptidase inhibitor *N*-ethylmaleimide (0.5 mM). Cell lysates were precleared with control IgG for 3 h at 4 °C, and then incubated with anti-XIAP mAb (Santa Cruz) overnight at 4 °C. Immunoprecipitates were washed three times and analyzed by immunoblot analysis.

The samples were subjected to SDS-PAGE and transferred onto PVDF membranes. The membranes were probed with the following antibodies: anti-STAMBPL1 (SAB4200145, Sigma), anti-GAPDH (sc-32233, Santa Cruz -biotechnology), anti-PARP (#9542, CST), anti-caspase 3 (#9665, CST), anti-caspase 7 (#12827, CST), anti-caspase 8 (#9746, CST), anti-caspase 9 (#9502, CST), anti-IκBα (#4812, CST), anti-phospho-IκBα (Ser32) (#2859, CST), anti-NF-κB p65 (#8242, CST), anti-XIAP (#2045, CST), anti-XIAP (sc-55552, Santa Cruz), anti-ubiquitin (#3933, CST) or anti-c-IAP1 (#7065, CST).

2.6. Flow cytometry, caspase activity

Cell death was determined by PI exclusion (Invitrogen P3566). Cells were collected and stained with 1 μg/mL of PI in PBS containing. For DNA content assay, cells were fixed with 70% ethanol at −20 °C for 24 h, then washed and stained with 50 μg/ml of PI, treated with RNase A for 30min. For apoptosis assay, cells were harvested and re-suspended in Annexin V binding buffer and incubated with FITC Annexin V and PI following the protocol of FITC Annexin V Apoptosis Detection Kit I (556547, BD Biosciences). For ROS analysis, cells were incubated either with H2DCFDA (25 μM), C11-BODIPY (581/591) (2 μM) or MitoSOX (5 μM) for 30 min at 37 °C. Cells were acquired and analyzed on BD FACsCalibur system with CellQuest Pro software. Caspase-3/7 or caspase 8 activity was measured using the Caspase-Glo 3/7or Caspase-Glo 8 or Assay kits (Promega).

2.7. Real-time PCR

Total RNA was extracted using Trizol reagent (Invitrogen). 1 μg of purified RNA/sample was reverse-transcribed using random hexamers as primers according to the Tetro cDNA synthesis kit (Bioline). qPCR was performed with the iTaq universal SYBR green supermix (Bio-rad). Data were analyzed by the 2-ΔΔCT method for relative quantification. Experimental Ct values were normalized to GAPDH levels and relative mRNA expression was calculated versus a control sample. The primers used for qPCR were: A20: 5′-CTGCCCAGGAATGCTACAGATAC-3′ and 5′-GTGGAACAGCTCGGATTTCAG-3'; COX2: 5′-CACCCATGTCAAAACC GAGG-3′ and 5′-CCGGTGTTGAGCAGTTTTCTC-3'; IκBα: 5′-GATCC-GCCAGGTGAAGGG-3′ and 5′-GCAATTTCTGGCTGGTTGG-3'; IL6: 5′-AATTCGGTACATCCTCGAC-GG-3′ and 5′-GGTTGTTTTCTGCC-AGT-

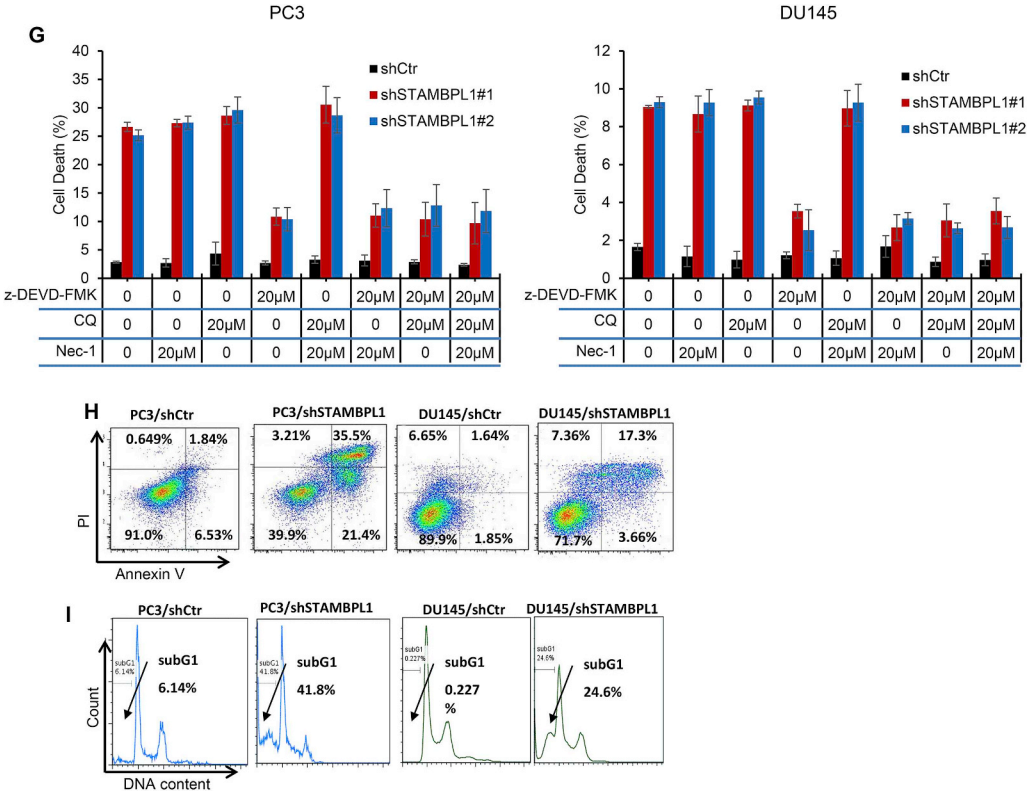

Fig. 1. (*continued*)

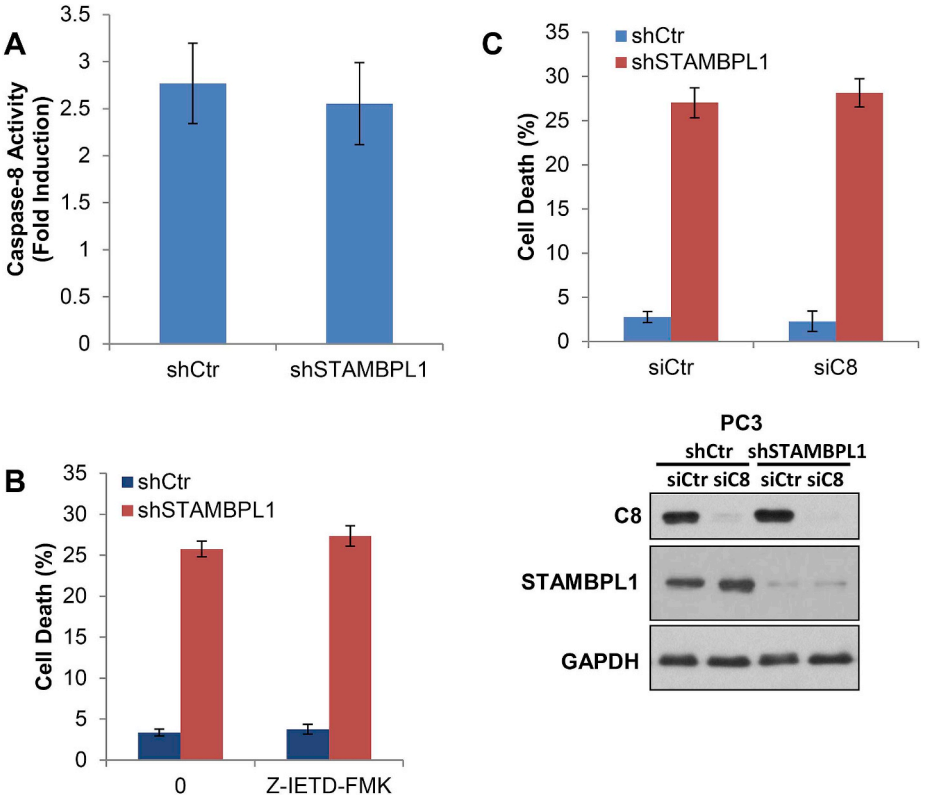

Fig. 2. STAMBPL1 depletion-induces apoptosis is independent of caspase 8 activation.
A. PC3 cells were infected with control shRNA or STAMBPL1shRNA for 48 h. Cells were assayed for caspase-3/7 activity.
B. PC3 cells were infected with indicated shRNAs for 24 h, and treated with 100 μM Z-IETD-FMK for 24 h. Cell death was analyzed by PI exclusion assay.
C. Upper panel. PC3 cells were infected with indicated shRNAs and transfected with control siRNA or siRNA against caspase 8 for 48 h. Cell death was analyzed as in B. Lower panel. Immunoblotting confirmed the knockdown efficiency of RNAi.

GCC-3'; XIAP: 5′-AGCCAAGGGGAA-TGAAGTGA-3′ and 5′-GGGGA-AGG-GCATTTGAAGAA-3'; STAMBPL1: 5′-GAGGATGGCGTCTGTGTAT TTG-3′ and 5′-GCTGGTAATCTCGATGGTTAGG-3'; GAPDH: 5′-CATGG GTGTGAACCATGAGA-3′ and 5′-CAGTGATGGCATGGACTG-TG-3'.

2.8. Statistical analysis

Statistical analysis was performed using student's t-test and one-way ANOVA. Results are expressed as mean ± standard deviation of at least three independent experiments. The overall survival was

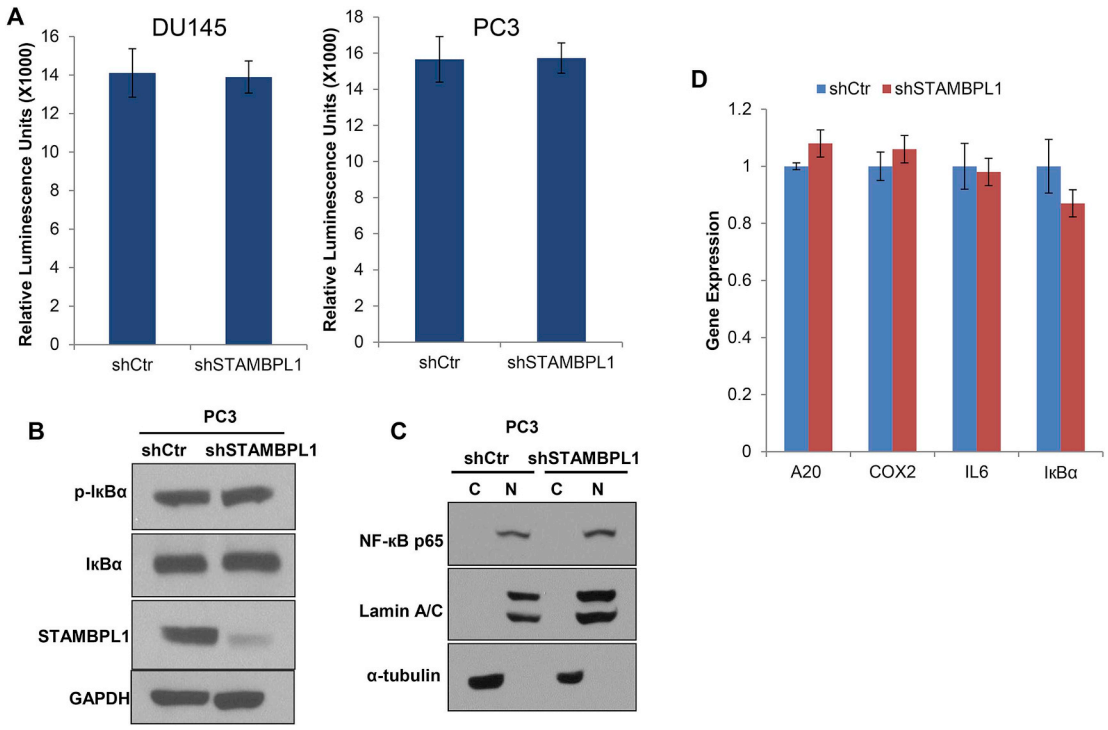

Fig. 3. STAMBPL1 does not regulate NF-kB activation.
A. DU145 and PC3 cells were infected with control shRNA or STAMBPL1shRNA, and transfected a NF-B firefly luciferase reporter plasmid for 48 h. Luminescence was measured using the Pierce Gaussia luciferase flash assay kit.
B, C and D. PC3 cells were infected with indicated shRNAs for 48 h. Total cell lysates were analyzed by IB (B). NF-kB p65 expression in nuclear extracts (N) and cytosolic (C) was determined by IB. Lamin A/C and α-tubulin were used as loading controls for each fraction (C). NF-kB -responsive genes were analyzed by qPCR.

examined with the Kaplan-Meier method and compared with the log-rank test. P-values of < 0.05 were considered to be significant.

3. Results

3.1. STAMBPL1 knockdown leads to apoptosis in DU145 and PC3 cells

We analyzed the genetic alteration of STAMBPL1 in different types of human prostate cancers from TCGA database of sample size n > 100 (http://www.cbioportal.org). The gene alteration frequency of STAMBPL1 is generally < 11% in prostate cancers (Fig. 1A). Amplification is the most common genetic alteration in neuroendocrine prostate cancers (7.89% of 114 samples) [22], but also in prostate adenocarcinomas (0.4% of 499 samples) [23]. We interrogated the GEPIA to explore the relative expression of STAMBPL1 mRNA levels in normal versus tumor tissues using TCGA prostate adenocarcinoma (PRAD) dataset. STAMBPL1 mRNA levels were higher in primary prostate cancer tissues compared to normal tissues (Fig. 1B). To evaluate if high STAMBPL1 mRNA expression was relevant to patient survival, we analyzed the overall survival correlation with STAMBPL1 gene expression data from prostate adenocarcinoma study performed by TCGA. Patients were divided into Low STAMBPL1 and High STAMBPL1 groups in respect to the median value. The patients overall survival plot revealed that patients with higher expression of STAMBPL1 gene had worse overall survival, suggesting a correlation between high levels of STAMBPL1 and an unfavorable prognosis (Fig. 1C). Based on bioinformatics analysis results, we investigated the biological effect of STAMBPL1 in prostate cancer cells. Substantially high levels of STAMBPL1 expression were detected in highly aggressive and androgen independent prostate cancer PC3, DU145, 22RV1 cells, as compared with androgen dependent LNCaP prostate cancer cells, LNCaP-derived, androgen-insensitive C4-2 cells and RWPE-1 normal prostate cells by immunoblotting (Fig. 1D and Supplementary Fig. 1A). Since the differential expression of STAMBPL1 in androgen-insensitive and –sensitive cells, we next asked whether *STAMBPL1* is one of the androgen-regulated gene. To that end, we treated androgen sensitive LNCaP cells with androgen receptor antagonist enzalutamide in either regular culture medium or androgen-depleted medium, and examined STAMBPL1 protein level and mRNA level. As shown in Supplementary Figs. 1B and C, antiandrogen treatment did not change the expression of STAMBPL1 in LNCaP cells, indicating *STAMBPL1* might not be an androgen responsible gene.

To address the basis for STAMBPL1 effect in prostate cancer, we silenced STAMBPL1 and examined cell viability. Two different specific shRNAs against STAMBPL1 (shSTAMBPL1#1 and #2) were used to exclude the possibility of off-target effects. Immnunoblotting confirmed effective STAMBPL1 knockdown by shRNAs (Fig. 1E). Interestingly, knockdown of endogenous STAMBPL1 markedly induced PC3 and DU145 cell death (Fig. 1F), indicating that STAMBPL1 is required for PC3 and DU145 cells survival. We also knocked down STAMBPL1 in 22RV1, C4-2 and LNCaP cells, we did not observe cell death in these three cell lines (Supplementary Fig. 1D), albeit the expression level of STAMBPL1 is much higher in 22RV1 cells than that in LNCaP and C4-2 cells.

Previous studies have reported that K63 ubiquitination of RIPK1 is a critical event in the process of necroptosis [24–26]. Accumulated evidences have been reported the essential role of K63 polyubquitin chains in the regulation of apoptosis [1] and autophagic cell death [27,28]. STAMBPL1 is a deubiquitinase enzyme, which specifically cleaves K63-linked polyubiquitin chains [6,7], although the substrates of STAMBPL1 are not well defined. To elucidate the machinery of STAMBPL1 depletion-induced cell death, we tested necroptosis inhibitor necrostatin-1 (Nec-1), autophagy inhibitor chloroquine (CQ) and caspase 3 inhibitor Z-DEVD-FMK for their ability to suppress cell death induced by STAMBPL1 knockdown. We infected PC3 and DU145 cells with shSTAMBPL1 lentivirus and treated cells with a series combination of

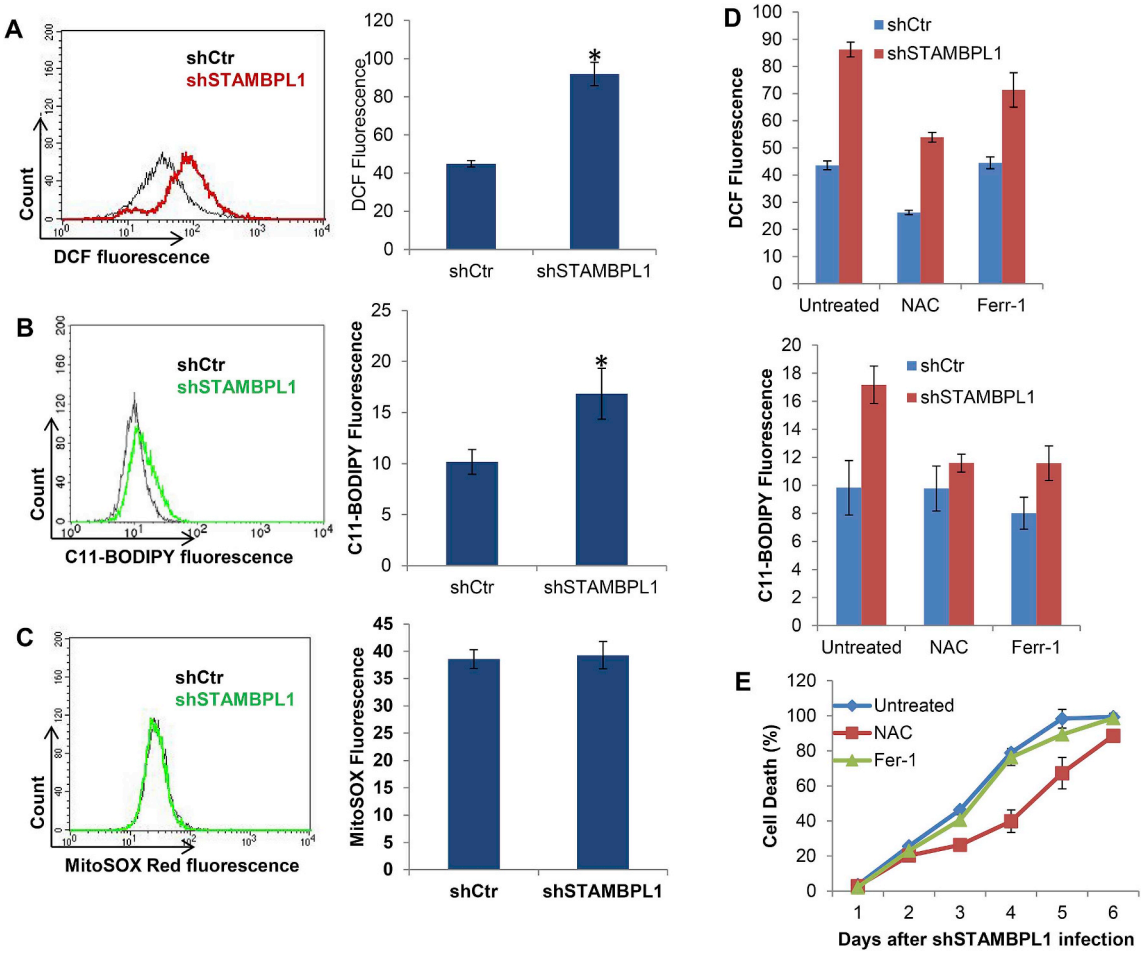

Fig. 4. ROS are required for STAMBPL1 depletion-induced apoptosis.
A, B, and C. PC3 cells were infected with indicated shRNAs for 48 h. Cytosolic, lipid and mitochondrial ROS were assessed by flow cytometry using H2DCFDA (A) and C11-BODIPY (B) and MitoSOX red (C) respectively.
D. PC3 cells were infected with indicated shRNAs for 48 h. Cells were treated with NAC (5 mM) or Fer-1 (10 μM) for 24 h. Cytosolic and lipid were assessed by flow cytometry. E. Cells were treated as in D. Cell viability over time was assessed by PI exclusion assay. (For interpretation of the references to colour in this figure legend, the reader is referred to the Web version of this article.)

Nec-1, CQ and Z-DEVD-FMK. Necroptosis inhibitor Nec-1 and autophagy inhibitor CQ did not efficiently suppress cell death induced by STAMBPL1 targeting; whereas, addition of a caspase 3 inhibitor, Z-DEVD-FMK, to cells markedly attenuated cell death (Fig. 1G), indicating a possible role of STAMBPL1 in regulating apoptosis signaling.

To further test whether STAMBPL1 depletion triggers apoptosis signaling, we assessed apoptotic cell death by Annexin V/PI staining and sub-G1 peak assay. STAMBPL1 knockdown in both PC3 and DU145 cells significantly increased Annexin V-positive cell population (Fig. 1H), as well as accumulation of dead cells in sub-G1 phase (Fig. 1I). We examined the cleavage of poly (ADP-ribose) polymerase (PARP), caspase −3, −7 and −9, the biochemical hallmarks of apoptosis signaling. The abundance of PARP, caspase-3, -7 and -9 cleavage products was observed in STAMBPL1-delpleted cells (Fig. 1J). Consist with these data, STAMBPL1 depletion resulted in a 4-fold increase in caspase-3/-7 enzymatic activity (Fig. 1K). Taken together, these data indicate that inhibition of STAMBPL1 in prostate cancer cells triggers caspase-dependent apoptosis.

3.2. Caspase 8 is not required for STAMBPL1 depletion induced apoptosis

Considering that caspase 8 is the predominant initiator caspase in the cell-extrinsic apoptosis pathway [29] and plays a pivotal role in unfolded-protein-response induced apoptosis [30,31], we wondered whether caspase 8 mediated STAMBPL1 loss-induced cell death. We noticed that the cleavage of caspase 8 was undetectable, and the total cellular amount of caspase 8 was not appreciably changed in STAMBPL1 knockdown cells (Fig. 1J). Caspase 8 activity was not elevated in both control shRNA and shSTAMBPL1 cells (Fig. 2A). Moreover, pharmaceutically or genetically silencing caspase 8 by z-IETD-FMK or siRNA against caspase 8 did not inhibit apoptosis activation by STAMBPL1 depletion (Fig. 2B and C). These data ruled out the dependence of cell death on caspase 8 activation, indicating cell-extrinsic pathway is not a mechanism underlying the STAMBPL1 depletion induced apoptosis.

3.3. STAMBPL1 is not a potential regulator of NF-kB activation in prostate cancer cells

It was reported that STAMBPL1 positively regulates NF-kB signaling by promoting human T-cell leukemia virus type I Tax nuclear export [32]. As NF-kB is a prominent feature of PC3 and DU145 androgen-independent cell lines [33,34], we investigated the role of STAMBPL1 in the maintenance of NF-kB activation. PC3 and DU145 cells were knocked down STAMBPL1 and transfected with NF-kB luciferase reporter. In line with previous report [32], silencing of STAMBPL1 had no effect on NF-kB luciferase activity as compared (Fig. 3A). NF-kB is retained in the cytoplasm with inhibitory IkB proteins. Upon activation,

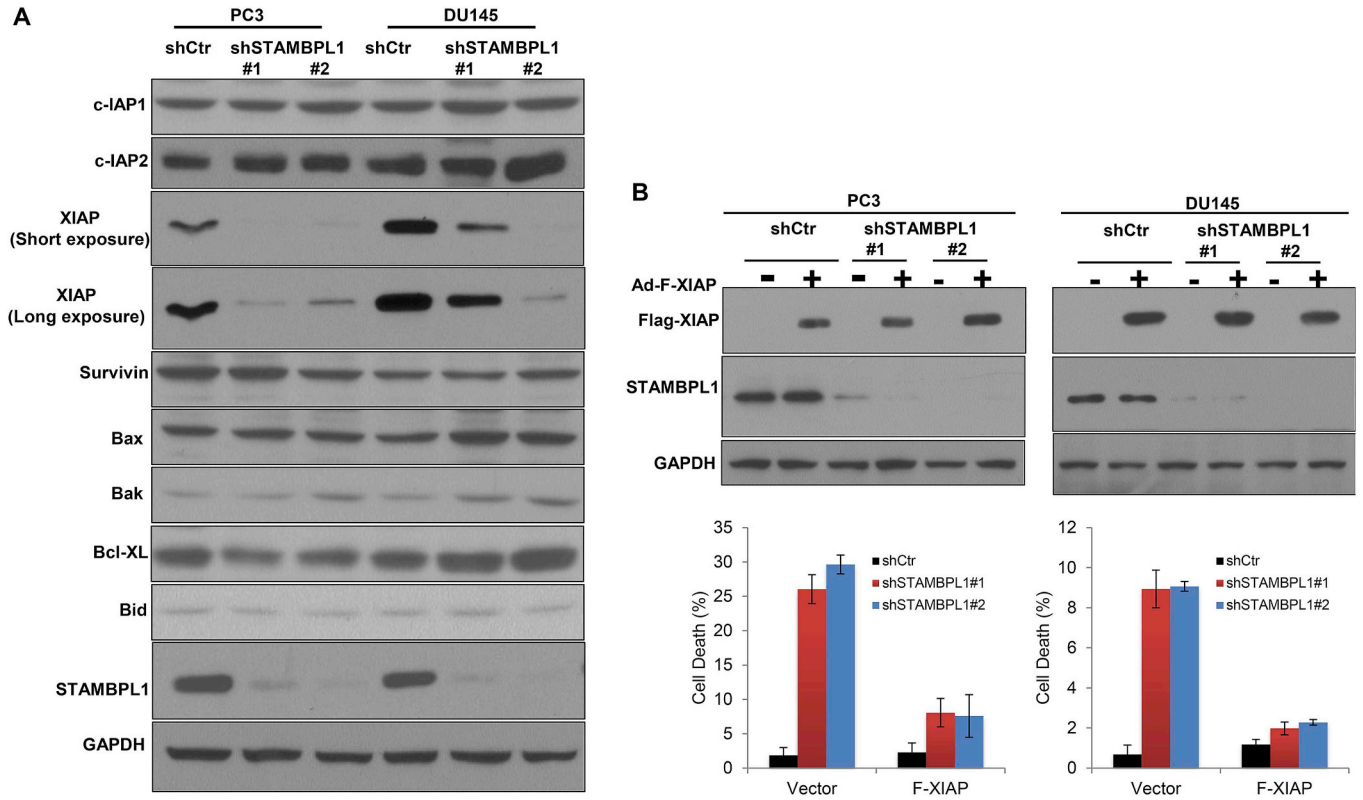

Fig. 5. XIAP loss mediates STAMBPL1 depletion-induced apoptosis.
A. PC3 and DU145 cells were infected with indicated shRNAs for 48 h. Protein abundance was analyzed by IB of total cell lysate.
B. PC3 and DU145 cells were infected with indicated shRNAs along with Ad-vector or Ad-Flag-XIAP for 48 h. Upper panel: Overexpression of XIAP was confirmed by IB; Lower panel: Cell death was measured by PI exclusion assay.

NF-kB is released from phosphorylated IkBa and is subsequently translocated into nucleus where it transcriptionally activates anti-apoptosis genes [35]. Although phosphorylated IkBa and nuclear NF-kB were highly expressed under normal cell culture condition, we did not observe a difference in their protein levels between control cells and STAMBPL1 silenced cells (Fig. 3B and C). Moreover, we examined NF-kB responsive genes using qPCR, and observed that STAMBPL1 knockdown did not change COX2, IκBα, A20, and IL6 mRNA levels (Fig. 3D).

3.4. ROS are non-redundant for STAMBPL1depletion-induced apoptosis

Previous studies showed that oxidative stress is inherent in prostate cancer cells [36]. However, excessive cellular reactive oxygen species (ROS) cause apoptosis via mitochondria pathway [37]. To determine whether STAMBPL1 depletion induced apoptosis is through oxidative stress, we measured cytosolic and lipid ROS by flow cytometry using the fluorescent probes H2DCFDA and C11-BODIPY. Compared to the control cells, STAMBPL1 knockdown cells showed 1.2-fold accumulation of cellular ROS, and 0.7-fold induction of lip ROS (Fig. 4A and B). In an effort to search the source of ROS accumulation, we stained cells with MitoSOX, a mitochondrial superoxide indicator, to test whether the aberrant ROS production was from the mitochondrial electron transport chain (ETC). However, no increase of MitoSOX-sensitive ROS production was found in STAMBPL1 depleted cells (Fig. 4C), indicating mitochondrial ROS was not evoked by STAMBPL1 depletion. To test whether oxidative stress was major mechanism of cell death, we treated cells with either antioxidant N-acetyl cysteine (NAC) or a lipid ROS scavenger ferrostatin-1 (Fer-1) [38]. As shown in Fig. 4D, ROS was markedly reduced by NAC or Fer-1. However, NAC treatment delayed, but did not rescue cell death, while Fer-1 had no effect on cell death (Fig. 4E). These results indicate that ROS accumulation is insufficient for maximal apoptosis in STAMBPL1-depleted cells.

3.5. XIAP levels determine apoptosis induced by STAMBPL1 depletion

To determine the mechanism of STAMBPL1 depletion-induced apoptosis, we sought to monitor amounts of several pro- and anti-apoptotic factors. Knockdown of STAMBPL1 in PC3 and DU145 cells had no effect on the abundance of Bax, Bak, Bid, Bcl-xl, c-IAP1/2, or survivin; only X-linked inhibitor of apoptosis (XIAP) was significantly declined (Fig. 5A). Since XIAP is the most potent inhibitor of caspase-3/-7 and −9, and serves as an important guardian against cell death [39,40], we tested whether XIAP is responsible for the apoptosis of STAMBPL1-silenced cells. We overexpressed XIAP and knocked down STAMBPL1 in PC3 and DU145 cells. Strikingly, overexpression of XIAP drastically reduced the extent to which PC3 and DU145 cells apoptosed when STAMBPL1 was depleted, and eliminated the difference in the levels of cell death between control and STAMBPL1 silenced cells (Fig. 5B). These results suggest that apoptosis by STAMBPL1 depletion results from loss of antiapoptotic protein XIAP.

3.6. STAMBPL1 promotes XIAP through lysosomal degradation

To dissect how STAMBPL1 regulates XIAP abundance, we analyzed XIAP mRNA levels in control and STAMBPL1 knockdown cells by qPCR. Albeit the sharp drop seen in XIAP protein level in STAMBPL1 depleted cells, we did not observe any change in XIAP mRNA level (Fig. 6A), indicating that regulation of XIAP expression by STAMBPL1 is mediated via posttranslational mechanism.

As XIAP protein is degraded through the proteasomal and/or lysosomal pathways [41,42], we treated cells with either proteasome inhibitor MG132 or lysosome inhibitor leupeptin and compared XIAP protein over time. Suppression of proteasome or lysosome restored

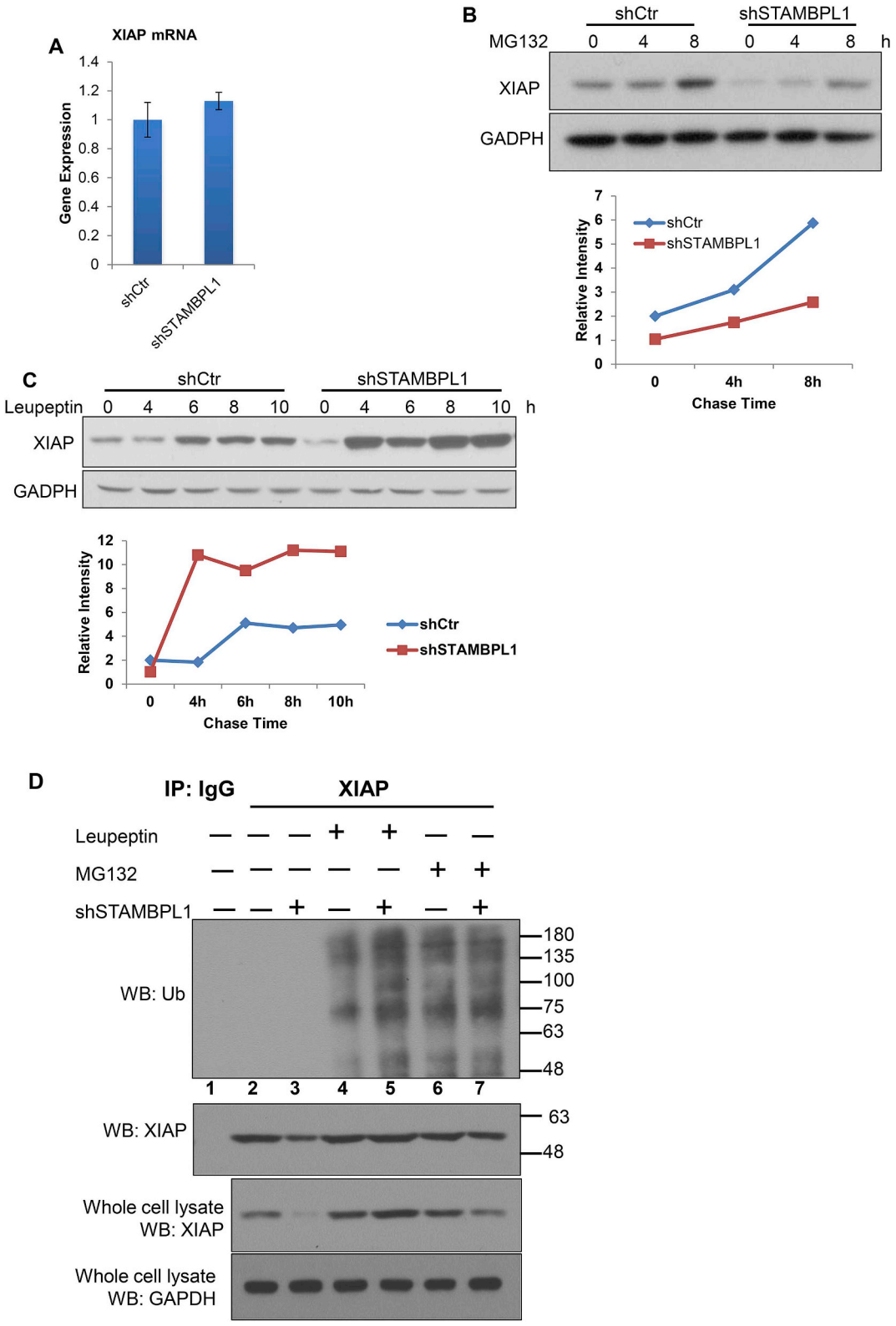

Fig. 6. STAMBPL1 regulates lysosomal degradation of XIAP.

A. Relative XIAP mRNA level was measured by qPCR in PC3 cells infected with indicated shRNAs.

B and C. PC3 cells received indicated shRNAs were treated MG132 (10 μM) or leupeptin (50 μM) for the indicated hours. Cell lysates were immunoblotted for XIAP or GAPDH.

D. PC3 cells received with indicated shRNAs were treated with MG132 (10 μM) or leupeptin (50 μM) for 8 h. Cell lysates were immunoprecipitated using anti-XIAP antibody, and blotted with anti-ubiquitin (UB) and anti-XIAP antibodies. Molecular weight markers (in kDa) are indicated on the right.

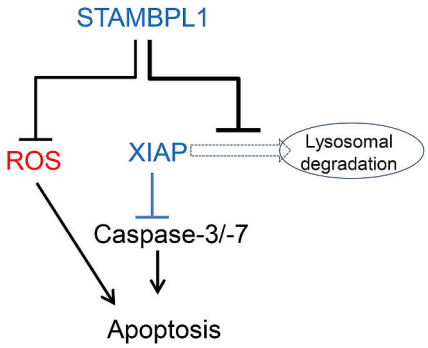

Fig. 7. Proposed model for the role of STAMBPL1 in regulation apoptosis pathway.
STAMBPL1 inhibits the lysosomal degradation of XIAP and cellular ROS production to promote prostate cancer cell survival.

XIAP in PC3 cells indicating XIAP could be destroyed through both pathways (Fig. 6B and C). Nevertheless we observed a different pattern in XIAP accumulation in control and STAMBPL1 cells treated with MG132 or leupeptin. XIAP level was much lower in shSTAMBPL1 cells than that in control cells, MG132 treatment did not bring XIAP protein to the similar level as in control cells, indicating STAMBPL1 is unlikely to be involved in the dynamic of XIAP proteasomal degradation. In contrast, leupeptin treatment elevated XIAP level in shSTAMBPL1 cells to the maximum, which was much higher than that in leupeptin-treated control cells. To study the effect of STAMBPL1 on the ubiquitination status of XIAP, PC3 cells were infected shCtr or shSTAMBPL1 lenti-virus follow by treatment with leupeptin or MG312 for 8 h. XIAP was pulled down by anti-XIAP monoclonal antibody and the extent of ubiquitination was analyzed by using anti-ubiquitin antibody. Inhibition of lysosome activity by leupeptin induced weaker ubiquitination of XIAP than the inhibition of lysosome activity by MG132 in shRNA control cells (Fig. 6 D, lanes 4 and 6), indicating that XIAP decay in control was mainly through proteasome degradation pathway. Of note, leupeptin treatment profoundly elevated XIAP ubiquitination in STAMBPL1 knockdown cells, MG132 treatment resulted in a similar pattern of ubiquitination of XIAP in both shCtr cells and shSTAMBPL1 cells (Fig. 6D, lanes 5 and 7), indicating that knocking down STAMBPL1 enhanced lysosomal degradation of XIAP. These data suggest that STAMBPL1 loss diverts the XIAP degradation from proteasome pathway to lysosome pathway, and drastically enhances XIAP degradation.

4. Discussion

In this study, we reported evidence that silencing STAMBPL1 by shRNA induced apoptosis in androgen-insensitive prostate cancer PC3 and DU145 cells, uncovering a previously unknown role for STAMBPL1 in controlling apoptosis signal in prostate cancer. We proposed the regulatory role of STAMBPL1 in apoptosis repertoire (Fig. 7).

The currently mainstay treatment of prostate cancer is androgen ablation therapy which is initially very effective at suppressing tumor [43]. However, long term androgen deprivation (12–33 months) often results in androgen resistance, leading to androgen-insensitive prostate cancer which is accompanied by genotypic and phenotypic alteration in several signaling pathway [44]. Therefore, targeting the key molecule (s) during the progression to androgen resistance may shed light on the development of novel therapeutic strategies towards prostate cancer. Although STAMBPL1 has been identified as a deuibiquitinase for more than a decade [5,6], its function is still unclear. In an effort to elucidate the potential role of STAMBPL1 in prostate cancer, we compared the STAMBPL1 protein levels in several prostate cancer cells. The finding that STAMBPL1 is highly expressed in androgen insensitive PC3 and DU145 cells, not in androgen-sensitive LNCaP cell [45] and immortalized prostatic PWE cells [19], prompted us to investigate whether STAMBPL1 is required for androgen insensitive cell survival. Of interest, PC3 and DU145 cells underwent apoptosis when STAMBPL1 was knocked down by shRNA. We focused on apoptosis pathway in our following experiments.

Sequential activation of caspase family is the key event for both intrinsic and extrinsic apoptosis pathways. Activation of initiator caspase-8 by ligands binding to cell surface death receptors can either directly cleave executioner caspas-3/-7, or activate intrinsic apoptosis by cleaving BID, depending on the cell type [39,40,46]. We observed activation of caspase-9, -3 and -7, but not caspase-8, in STAMBPL1 silencing-induced apoptosis. We further excluded the role of caspase-8 in STAMBPL1-dependent process, as pharmaceutically or genetically inhibiting caspase-8 did not affect cell death, indicating STAMBPL1 silencing triggers intrinsic apoptotic signal. Knocking down STAMBPL1 also promoted a burst of cellular ROS, which is non-redundant, but not sufficient to induce efficient cell death. We have not completely ruled out the involvement of ROS in apoptosis, nor the possibility that ROS alter regulators involving apoptosis. Additional studies are required to investigate the source of ROS. Consistent with a previous study [32], STAMBPL1 does not regulate endogenous NF-κB activation and NF-κB downstream transcription.

To decipher STAMBPL1's role in apoptosis repertoire, we examined IAP family protein levels in STAMBPL1-silenced cells. Of interest, XIAP protein was diminished by STAMBPL1 RNAi. Structural and biochemical analyses have shown that XIAP directly blocks the proteolytic activity of caspase-3/-7 and −9 [47], we reasoned that the effect of STAMBPL1 RNAi on the activation of caspase-3/-7 and −9 resulted from the loss of XIAP. Accordingly, overexpression of XIAP in STAMBPL1-silenced cells rescued cell death, supporting the notion that decreasing XIAP is the major mechanism underlying the cell death caused by STAMBPL1 downregulation. Accumulating evidence showed that many other deubiquitinases regulate key apoptotic regulators, including IAPs, and also control protein half-life by the removal ubiquitin from target proteins [1,2]. As having shown STAMBPL1 has no effect on XIAP mRNA level, we examined XIAP degradation by treating cells with either protease inhibitor MG132 or lysosome inhibitor leupeptin, and observed that STAMBPL1 knockdown exacerbated XIAP degradation through lysosomal pathway. We observed that STAMBPL1 depletion modulates XIAP ubiquitination status, which diverts the XIAP degradation from proteasome pathway to lysosome pathway. Future studies will be required to investigate whether XIAP is a substrate of STAMBPL1, how XIAP can be regulated by Lys-63 linked ubiquitination.

Conflicts of interest

None.

Acknowledgments

This work was partially supported by the President's Fund of Nanfang Hospital, Southern Medical University (No. 2017L002).

Appendix A. Supplementary data

Supplementary data to this article can be found online at https://doi.org/10.1016/j.canlet.2019.04.020.

References

[1] D. Vucic, V.M. Dixit, I.E. Wertz, Ubiquitylation in apoptosis: a post-translational modification at the edge of life and death, Nat. Rev. Mol. Cell Biol. 12 (2011) 439–452.
[2] S. Ramakrishna, B. Suresh, K.H. Baek, The role of deubiquitinating enzymes in apoptosis, Cell. Mol. Life Sci.: CMLS 68 (2011) 15–26.
[3] K. Husnjak, I. Dikic, Ubiquitin-binding proteins: decoders of ubiquitin-mediated cellular functions, Annu. Rev. Biochem. 81 (2012) 291–322.

[4] D. Mukhopadhyay, H. Riezman, Proteasome-independent functions of ubiquitin in endocytosis and signaling, Science (New York, N.Y.) 315 (2007) 201–205.
[5] K. Kikuchi, N. Ishii, H. Asao, K. Sugamura, Identification of AMSH-LP containing a Jab1/MPN domain metalloenzyme motif, Biochem. Biophys. Res. Commun. 306 (2003) 637–643.
[6] Y. Sato, A. Yoshikawa, A. Yamagata, H. Mimura, M. Yamashita, K. Ookata, O. Nureki, K. Iwai, M. Komada, S. Fukai, Structural basis for specific cleavage of Lys 63-linked polyubiquitin chains, Nature 455 (2008) 358–362.
[7] J. McCullough, M.J. Clague, S. Urbe, AMSH is an endosome-associated ubiquitin isopeptidase, J. Cell Biol. 166 (2004) 487–492.
[8] M.S. Kim, J.A. Kim, H.K. Song, H. Jeon, STAM-AMSH interaction facilitates the deubiquitination activity in the C-terminal AMSH, Biochem. Biophys. Res. Commun. 351 (2006) 612–618.
[9] T.K. Oberoi-Khanuja, A. Murali, K. Rajalingam, IAPs on the move: role of inhibitors of apoptosis proteins in cell migration, Cell Death Dis. 4 (2013) e784.
[10] D.B. Seligson, F. Hongo, S. Huerta-Yepez, Y. Mizutani, T. Miki, H. Yu, S. Horvath, D. Chia, L. Goodglick, B. Bonavida, Expression of X-linked inhibitor of apoptosis protein is a strong predictor of human prostate cancer recurrence, Clin. Cancer Res.: Off. J. Amer. Assoc. Canc. Res. 13 (2007) 6056–6063.
[11] J.M. Cummins, M. Kohli, C. Rago, K.W. Kinzler, B. Vogelstein, F. Bunz, X-linked inhibitor of apoptosis protein (XIAP) is a nonredundant modulator of tumor necrosis factor-related apoptosis-inducing ligand (TRAIL)-mediated apoptosis in human cancer cells, Cancer Res. 64 (2004) 3006–3008.
[12] R.L. Siegel, K.D. Miller, A. Jemal, Cancer statistics, CA A Cancer J. Clin. 67 (2017) 7–30 2017.
[13] R. Zheng, H. Zeng, S. Zhang, T. Chen, W. Chen, National estimates of cancer prevalence in China, Cancer Lett. 370 (2011) 33–38 2016.
[14] W. Chen, R. Zheng, P.D. Baade, S. Zhang, H. Zeng, F. Bray, A. Jemal, X.Q. Yu, J. He, Cancer statistics in China, 2015, CA A Cancer J. Clin. 66 (2016) 115–132.
[15] P. Saraon, K. Jarvi, E.P. Diamandis, Molecular alterations during progression of prostate cancer to androgen independence, Clin. Chem. 57 (2011) 1366–1375.
[16] P. Saraon, A.P. Drabovich, K.A. Jarvi, E.P. Diamandis, Mechanisms of androgen-independent prostate cancer, Ejifcc 25 (2014) 42–54.
[17] S.B. Howell, Resistance to apoptosis in prostate cancer cells, Mol. Urol. 4 (2000) 225–229 discussion 231.
[18] P.I. Lorenzo, Y.J. Arnoldussen, F. Saatcioglu, Molecular mechanisms of apoptosis in prostate cancer, Crit. Rev. Oncog. 13 (2007) 1–38.
[19] D. Bello, M.M. Webber, H.K. Kleinman, D.D. Wartinger, J.S. Rhim, Androgen responsive adult human prostatic epithelial cell lines immortalized by human papillomavirus 18, Carcinogenesis 18 (1997) 1215–1223.
[20] Z. Tang, C. Li, B. Kang, G. Gao, C. Li, Z. Zhang, GEPIA: a web server for cancer and normal gene expression profiling and interactive analyses, Nucleic Acids Res. 45 (2017) W98–W102.
[21] S. Mohapatra, B. Chu, X. Zhao, W.J. Pledger, Accumulation of p53 and reductions in XIAP abundance promote the apoptosis of prostate cancer cells, Cancer Res. 65 (2005) 7717–7723.
[22] H. Beltran, D. Prandi, J.M. Mosquera, M. Benelli, L. Puca, J. Cyrta, C. Marotz, E. Giannopoulou, B.V. Chakravarthi, S. Varambally, S.A. Tomlins, D.M. Nanus, S.T. Tagawa, E.M. Van Allen, O. Elemento, A. Sboner, L.A. Garraway, M.A. Rubin, F. Demichelis, Divergent clonal evolution of castration-resistant neuroendocrine prostate cancer, Nat. Med. 22 (2016) 298–305.
[23] The molecular taxonomy of primary prostate cancer, Cell 163 (2015) 1011–1025.
[24] M.C. de Almagro, T. Goncharov, A. Izrael-Tomasevic, S. Duttler, M. Kist, E. Varfolomeev, X. Wu, W.P. Lee, J. Murray, J.D. Webster, K. Yu, D.S. Kirkpatrick, K. Newton, D. Vucic, Coordinated ubiquitination and phosphorylation of RIP1 regulates necroptotic cell death, Cell Death Differ. 24 (2017) 26–37.
[25] H. Wang, H. Meng, X. Li, K. Zhu, K. Dong, A.K. Mookhtiar, H. Wei, Y. Li, S.C. Sun, J. Yuan, PELI1 functions as a dual modulator of necroptosis and apoptosis by regulating ubiquitination of RIPK1 and mRNA levels of c-FLIP, Proc. Natl. Acad. Sci. U. S. A. 114 (2017) 11944–11949.
[26] A. Annibaldi, S. Wicky John, T. Vanden Berghe, K.N. Swatek, J. Ruan, G. Liccardi, K. Bianchi, P.R. Elliott, S.M. Choi, S. Van Coillie, J. Bertin, H. Wu, D. Komander, P. Vandenabeele, J. Silke, P. Meier, Ubiquitin-mediated regulation of RIPK1 kinase activity independent of IKK and MK2, Mol. Cell 69 (2018) 566–580 e565.
[27] P. Grumati, I. Dikic, Ubiquitin signaling and autophagy, J. Biol. Chem. 293 (2018) 5404–5413.
[28] C. Gomez-Diaz, F. Ikeda, Roles of ubiquitin in autophagy and cell death, Seminars in Cell & Developmental Biology, 2018.
[29] A.B. Parrish, C.D. Freel, S. Kornbluth, Cellular mechanisms controlling caspase activation and function, Cold Spring Harb. Perspect. Biol. 5 (2013).
[30] Y. Estornes, M.A. Aguileta, C. Dubuisson, J. De Keyser, V. Goossens, K. Kersse, A. Samali, P. Vandenabeele, M.J. Bertrand, RIPK1 promotes death receptor-independent caspase-8-mediated apoptosis under unresolved ER stress conditions, Cell Death Dis. 5 (2014) e1555.
[31] J.A. Glab, M. Doerflinger, C. Nedeva, I. Jose, G.W. Mbogo, J.C. Paton, A.W. Paton, A.J. Kueh, M.J. Herold, D.C. Huang, D. Segal, G. Brumatti, H. Puthalakath, DR5 and caspase-8 are dispensable in ER stress-induced apoptosis, Cell Death Differ. 24 (2017) 944–950.
[32] A. Lavorgna, E.W. Harhaj, An RNA interference screen identifies the Deubiquitinase STAMBPL1 as a critical regulator of human T-cell leukemia virus type 1 tax nuclear export and NF-kappaB activation, J. Virol. 86 (2012) 3357–3369.
[33] R. Garg, J. Blando, C.J. Perez, H. Wang, F.J. Benavides, M.G. Kazanietz, Activation of nuclear factor kappaB (NF-kappaB) in prostate cancer is mediated by protein kinase C epsilon (PKCepsilon), J. Biol. Chem. 287 (2012) 37570–37582.
[34] G. Rodriguez-Berriguete, B. Fraile, R. Paniagua, P. Aller, M. Royuela, Expression of NF-kappaB-related proteins and their modulation during TNF-alpha-provoked apoptosis in prostate cancer cells, Prostate 72 (2012) 40–50.
[35] F. Wan, M.J. Lenardo, The nuclear signaling of NF-kappaB: current knowledge, new insights, and future perspectives, Cell Res. 20 (2010) 24–33.
[36] B. Kumar, S. Koul, L. Khandrika, R.B. Meacham, H.K. Koul, Oxidative stress is inherent in prostate cancer cells and is required for aggressive phenotype, Cancer Res. 68 (2008) 1777–1785.
[37] D.B. Zorov, M. Juhaszova, S.J. Sollott, Mitochondrial reactive oxygen species (ROS) and ROS-induced ROS release, Physiol. Rev. 94 (2014) 909–950.
[38] R. Skouta, S.J. Dixon, J. Wang, D.E. Dunn, M. Orman, K. Shimada, P.A. Rosenberg, D.C. Lo, J.M. Weinberg, A. Linkermann, B.R. Stockwell, Ferrostatins inhibit oxidative lipid damage and cell death in diverse disease models, J. Am. Chem. Soc. 136 (2014) 4551–4556.
[39] D.R. McIlwain, T. Berger, T.W. Mak, Caspase functions in cell death and disease, Cold Spring Harb. Perspect. Biol. 5 (2013) a008656.
[40] J. Yuan, A. Najafov, B.F. Py, Roles of caspases in necrotic cell death, Cell 167 (2016) 1693–1704.
[41] J.B. Garrison, R.G. Correa, M. Gerlic, K.W. Yip, A. Krieg, C.M. Tamble, R. Shi, K. Welsh, S. Duggineni, Z. Huang, K. Ren, C. Du, J.C. Reed, ARTS and Siah collaborate in a pathway for XIAP degradation, Mol. Cell 41 (2011) 107–116.
[42] N. Wang, Y. Feng, M. Zhu, F.M. Siu, K.M. Ng, C.M. Che, A novel mechanism of XIAP degradation induced by timosaponin AIII in hepatocellular carcinoma, Biochim. Biophys. Acta 1833 (2013) 2890–2899.
[43] M.A. Perlmutter, H. Lepor, Androgen deprivation therapy in the treatment of advanced prostate cancer, Rev. Urol. 9 (Suppl 1) (2007) S3–S8.
[44] P.A. Watson, V.K. Arora, C.L. Sawyers, Emerging mechanisms of resistance to androgen receptor inhibitors in prostate cancer, Nat. Rev. Canc. 15 (2015) 701–711.
[45] S. Marchiani, L. Tamburrino, G. Nesi, M. Paglierani, S. Gelmini, C. Orlando, M. Maggi, G. Forti, E. Baldi, Androgen-responsive and -unresponsive prostate cancer cell lines respond differently to stimuli inducing neuroendocrine differentiation, Int. J. Androl. 33 (2010) 784–793.
[46] K. Boland, L. Flanagan, J.H. Prehn, Paracrine control of tissue regeneration and cell proliferation by Caspase-3, Cell Death Dis. 4 (2013) e725.
[47] Q.L. Deveraux, E. Leo, H.R. Stennicke, K. Welsh, G.S. Salvesen, J.C. Reed, Cleavage of human inhibitor of apoptosis protein XIAP results in fragments with distinct specificities for caspases, EMBO J. 18 (1999) 5242–5251.